Essential role of protein kinase Bγ (PKBγ/Akt3) in postnatal brain development but not in glucose homeostasis

Oliver Tschopp[1], Zhong-Zhou Yang[1], Daniela Brodbeck[1], Bettina A. Dummler[1], Maja Hemmings-Mieszczak[2], Takashi Watanabe[3], Thomas Michaelis[3], Jens Frahm[3] and Brian A. Hemmings[1,*]

[1]Friedrich Miescher Institute for Biomedical Research, Maulbeerstrasse 66, CH-4058 Basel, Switzerland
[2]Novartis Pharma AG, Lichtstrasse 35, CH-4056, Basel, Switzerland
[3]Biomedizinische NMR Forschungs GmbH am Max-Planck-Institut für biophysikalische Chemie, 37070 Göttingen, Germany
*Author for correspondence (e-mail: brian.hemmings@fmi.ch)

Accepted 14 April 2005

Development 132, 2943-2954
Published by The Company of Biologists 2005
doi:10.1242/dev.01864

Summary

Protein kinase B is implicated in many crucial cellular processes, such as metabolism, apoptosis and cell proliferation. In contrast to *Pkbα* and *Pkbβ*-deficient mice, *Pkbγ*$^{-/-}$ mice are viable, show no growth retardation and display normal glucose metabolism. However, in adult *Pkbγ* mutant mice, brain size and weight are dramatically reduced by about 25%. In vivo magnetic resonance imaging confirmed the reduction of *Pkbγ*$^{-/-}$ brain volumes with a proportionally smaller ventricular system. Examination of the major brain structures revealed no anatomical malformations except for a pronounced thinning of white matter fibre connections in the corpus callosum. The reduction in brain weight of *Pkbγ*$^{-/-}$ mice is caused, at least partially, by a significant reduction in both cell size and cell number. Our results provide novel insights into the physiological role of PKBγ and suggest a crucial role in postnatal brain development.

Key words: *Pkbγ/Akt3* knockout, Brain development, Apoptosis

Introduction

Protein kinase B (PKB/Akt) is a second messenger-regulated kinase that has been implicated in many crucial cellular processes, such as glucose metabolism, transcription, cell proliferation, apoptosis, migration and growth (Brazil and Hemmings, 2001; Chan et al., 1999; Datta et al., 1999; Kandel and Hay, 1999; Scheid and Woodgett, 2001). Deregulation of PKB activity contributes to cell transformation and diabetes (Brazil and Hemmings, 2001; Nicholson and Anderson, 2002). In mammalian cells, three closely related isoforms of the PKB family have been identified and termed PKBα/Akt1, PKBβ/Akt2 and PKBγ/Akt3 (Brodbeck et al., 1999; Cheng et al., 1992; Jones et al., 1991a; Jones et al., 1991b; Masure et al., 1999; Nakatani et al., 1999). These proteins are products of three separate genes located on distinct chromosomes and are widely expressed with a few isoform-specific features (Altomare et al., 1998; Yang et al., 2003). All three members of the PKB family contain a highly conserved N-terminal pleckstrin homology (PH) domain, a central catalytic domain and a short C-terminal regulatory domain (Hanada et al., 2004).

PKB is activated by numerous stimuli, including growth factors, hormones and cytokines (Brazil and Hemmings, 2001; Chan et al., 1999; Datta et al., 1999). Activation of PKB occurs in response to signalling via phosphoinositide 3 kinase (PI3K) and requires the membrane-bound second messenger phosphatidylinositol-3,4,5-triphosphate [PtdIns(3,4,5)P_3 or PIP3] (Burgering and Coffer, 1995; Cross et al., 1995; Franke et al., 1995). The current model for PKB regulation proposes that PtdIns(3,4,5)P_3, generated following PI3K activation, interacts with the PH domain of PKB, recruiting the inactive kinase from the cytoplasm to the plasma membrane and promoting a conformational change that allows phosphorylation on two regulatory sites by upstream kinases at the plasma membrane. One of these critical phosphorylation sites resides in the activation loop of the kinase domain (Thr308 in PKBα) and the other is located in the C-terminal regulatory domain (Ser-473 in PKBα), termed the hydrophobic motif (Alessi et al., 1996; Brodbeck et al., 1999; Meier et al., 1997). The upstream kinase that phosphorylates Thr308 in the activation loop of the kinase domain of PKBα in a PIP3-dependent-manner has been identified and termed 3-phosphoinositide-dependent kinase 1 (PDK1) (Alessi et al., 1997; Stokoe et al., 1997). Thr308 phosphorylation is necessary and sufficient for PKB activation; however, maximal activation requires additional phosphorylation at Ser473 (Alessi et al., 1996; Yang et al., 2002a; Yang et al., 2002b). Several different protein kinases and mechanisms have been proposed for the phosphorylation of the hydrophobic motif (Brazil and Hemmings, 2001; Yang et al., 2002b).

Mice with targeted disruption of *Pkbα* and/or *Pkbβ* have been obtained recently with *Pkbα* mutant mice displaying an increased neonatal lethality and a reduction in body weight of ~30% (Chen et al., 2001; Cho et al., 2001b; Yang et al., 2003). Moreover, loss of *Pkbα* leads to placental hypotrophy with impaired vascularisation (Yang et al., 2003). By contrast, *Pkbβ*-deficient mice are born with the expected Mendelian ratio and exhibit a diabetes-like syndrome with elevated fasting plasma glucose, hepatic glucose output, peripheral insulin resistance and an compensatory increase of islet mass (Cho et

al., 2001a). Compared with *Pkbα* mutant mice, *Pkbβ*-deficient mice are only mildly growth retarded (Cho et al., 2001a; Garofalo et al., 2003). However, mice lacking both isoforms die after birth, probably owing to respiratory failure (Peng et al., 2003). *Pkbαβ* double mutant newborns display a severe reduction in body weight (≈50%), prominent atrophy of the skin and skeletal muscle, as well as impaired adipogenesis and delayed ossification.

Here, we report the generation and characterisation of mice with targeted disruption of the *Pkbγ* gene. Compared with *Pkbα*$^{-/-}$ and *Pkbβ*$^{-/-}$ mice, *Pkbγ* mutant mice display a distinct phenotype without increased perinatal mortality, growth retardation or altered glucose metabolism. However, loss of PKBγ profoundly affects postnatal brain growth. Brains from adult *Pkbγ* mutant mice show a dramatic reduction in size and weight. Taken together, our results reveal a novel and important physiological role for PKBγ in postnatal brain development.

Materials and methods

Targeted disruption of the Pkbγ gene by homologous recombination

An ~11-kb *Hin*dIII fragment was subcloned containing exons 4 and 5 of *Pkbγ*. A *Nco*I site was generated in exon 4 for insertion of a ~5-kb IRES-*lacZ*-Neo cassette. The targeting vector was linearised with *Sal*I and electroporated into 129/Ola ES cells. An external probe was used for ES cell screening following *Xba*I digestion. An internal probe and a *lacZ*-Neo probe were used to characterize ES clones positive for homologous recombination (data not shown). Correctly targeted ES cells were used to generate chimeras. Male chimeras were mated with wild-type C57BL/6 females to obtain *Pkbγ*$^{+/-}$ mice. *Pkbγ*$^{+/-}$ mice have been backcrossed twice with pure C57BL/6 mice and the progeny of *Pkbγ*$^{+/-}$ intercrosses have ~75% C57BL/6 genetic background. Progeny were genotyped by multiplex PCR with the following three primers: (1) *P35*, GGTTCTGTGGGAGGTA-GTTCTC; (2) Neo-2, GCAATCCATCTTGTTCAATGGCCG; and (3) E4γ, CCATCGGTCGGCTACGGCTTGG.

Quantitative real time PCR

The levels of PKB isoforms in wild-type and mutant mice were determined by quantitative Q-RT-PCR. The experiment was performed as described previously (Yang et al., 2003). Briefly, total RNA was purified using Trizol Reagent (Invitrogen). For the Q-PCR reaction, 50 ng total RNA was mixed with 5′ and 3′ primers, Taqman probe, MuLV reverse transcriptase, RNase inhibitor and the components of the TaqMan PCR reagent kit (Eurogentec) in a total volume of 25 μl following the TaqMan PCR reagent kit protocol.

Western blot analysis

For Western blot analysis, protein lysates were processed as previously described (Yang et al., 2003). PKB isoform-specific antibodies were obtained by immunizing rabbits with isoform-specific peptides as previously described (Yang et al., 2003). Antibodies against phospho-PKB (Ser473), phospho-GSK3α/β (Ser21/9), phospho-TSC2 (Thr1462) and phospho-p70S6K were purchased from Cell Signalling Technologies. Antibodies against p27 and ERK were purchased from Santa Cruz Biotechnology. The antibody against phospho-ERK (Thr202/Tyr204) was purchased from Promega and the Pan-Actin antibody was obtained from NeoMarkers. Western blots were scanned using a GS-800 BioRad densitometer with a resolution of 63.5 μm × 63.5 μm and bands were quantified using Proteomweaver 3.0.0.6 (Definiens).

Histological examination

For histological analysis, animals were perfused with phosphate-buffered saline and 4% paraformaldehyde in phosphate-buffered saline. Organs were dissected and kept in the same fixation solution overnight at 4°C. Samples were embedded in paraffin following dehydration in ethanol. Tissues were cut into 6 μm sections and stored for staining. For Haematoxylin-Eosin and Cresyl-Violet (Sigma) staining, sections were freed of paraffin and stained.

Cell number determination

To determine the number of cells in a whole brain, the DNA content was determined as described by Labarca and Paigen (Labarca and Paigen, 1980). This method is based on the enhancement of fluorescence after binding of bisbenzimid (Riedel-de Haen) to DNA. A linear standard curve (1-10 μg/ml) was prepared to calculate the DNA concentration. The relative cell size in posterior cortex was measured on plane-matched, parasagittal brain sections stained with DAPI (Biotium). Image-Pro® Plus (Media Cybernetics) was used to count the cell number and to calculate the mean area occupied by one cell. The relative cell size is expressed as percent of wild type.

In vivo magnetic resonance imaging (MRI)

MRI studies of 4-month-old female *Pkbγ* wild-type (n=5) and mutant mice (n=5) were performed at 2.35 T using a MRBR 4.7/400 mm magnet (Magnex Scientific, Abingdon, England) equipped with BGA20 gradients (100 mT m^{-1}) and a DBX system (Bruker Biospin, Ettlingen, Germany). For in vivo examinations, animals were anaesthetized (1.0-1.5% halothane in 70:30 N_2O:O_2) and treated as previously described (Natt et al., 2002). Briefly, radiofrequency (rf) excitation and signal reception were accomplished with use of a Helmholtz coil (∅ 100 mm) and a surface coil (∅ 20×12 mm), respectively. Three-dimensional T_1-weighted (rf-spoiled 3D FLASH, repetition time TR=17 mseconds, echo time TE=7.6 mseconds, flip angle 25°, measuring time 84 minutes) and T_2-weighted MRI data sets (3D fast spin-echo, TR/TE=3000/98 mseconds, measuring time 58 minutes) were acquired with an isotropic resolution of 117 μm. Volumetric assessments were obtained by analysing T_1-weighted images using software provided by the manufacturer (Paravision, Bruker Biospin, Ettlingen, Germany). After manually outlining the whole brain and the ventricular spaces in individual sections, respective areas were calculated (in mm^2), summed and multiplied by the section thickness.

Neuronal cell culture

E16.5 murine hippocampal neurons were isolated from timed matings. Cells were kept in culture for 7 days on polylysine coverslips coated with B27/Neurobasal (GIBCO Life Technologies). At day 7, cultures were treated with glutamate (15 mM/24 hours), staurosporine (50 nM/12 hours) or were left untreated. For the detection of apoptotic cells, five fixed cultures per genotype were stained using a TUNEL-assay (Roche) according to the manufacturer's instructions and counterstained with DAPI (Biotium). At least 200 cells per culture were counted and the percentage of apoptotic cells was calculated.

Glucose and insulin tolerance test

Mice were housed according to the Swiss Animal Protection Laws in groups with 12 hours dark/light cycles and with free access to food and water. All procedures were conducted with the approval of the appropriate authorities.

Random-fed and fasting blood glucose levels were determined in 5- to 6-month-old mice. Blood samples were collected from tail veins and glucose levels were determined using Glucometer Elite (Bayer). Mice (aged 5-6 months) were fasted overnight before the start of the glucose and insulin tolerance tests. Glucose (2 g/kg) was given orally to conscious mice. Insulin (1 U/kg) was administered by intraperitoneal injection to conscious mice. Blood samples were collected at indicated times from tail veins and glucose levels were determined using Glucometer Elite (Bayer). Blood glucose levels were expressed as percentage of initial value. Blood insulin levels

were measured with a Mouse ultra-sensitive insulin ELISA (Immunodiagnostic Systems).

Microarray analysis

Microarray analysis was performed using murine MOE430A GeneChips™ (Affymetrix). Total RNA (10 μg) was reverse transcribed using the SuperScript Choice system for cDNA synthesis (Life Technologies) and biotin-labelled cRNA generated using the Enzo BioArray High Yield RNA transcript labelling kit (Enzo Diagnostics) following the manufacturer's protocol. cRNA fragmentation and hybridisation were performed as recommended by Affymetrix. Expression data were calculated using the RMA algorithm from BioConductor (Irizarry et al., 2003). A gene was considered to be significantly altered in its expression if it had an Affymetrix change *P*-value of less than 0.003 for either increase or decrease in at least two-thirds of replicate comparisons and it had a minimum expression value of 100 in at least one condition. A fold-change threshold of 1.5 was then applied and the resulting genes were subjected to a one-way ANOVA with a *P*-value cut-off of 0.05. A Benjamini and Hochberg multiple testing correction and a Tukey post-hoc test were applied.

Statistical analysis

To compare body weight, brain weight and volume, brain/body weight ratio, DNA content, cell number and percentage of apoptotic cells between $Pkb\gamma^{+/+}$ and $Pkb\gamma^{-/-}$, an unpaired Students *t*-test was performed. *P* values under 0.05 were considered as significant and values below 0.01 as highly significant.

Results

Targeting strategy and confirmation of genotype

$Pkb\gamma^{-/-}$ mice were generated by targeted disruption of exon 4 as shown in (Fig. 1A). The ablation of *Pkbγ* was confirmed by PCR, Q-RT-PCR and Western blot analysis using brain tissue samples from *Pkbγ* wild-type ($Pkb\gamma^{+/+}$), heterozygous ($Pkb\gamma^{+/-}$) and mutant ($Pkb\gamma^{-/-}$) mice (Fig. 1B). Quantitative RT-PCR displayed complete ablation of the PKBγ mRNA in brain samples of *Pkbγ* mutant mice (n=3, data not shown). To confirm the absence of PKBγ at the protein level, Western blot analysis was performed with an isoform-specific anti-PKBγ antibody. In contrast to $Pkb\gamma^{+/+}$ brain tissue samples, PKBγ was not detectable in samples derived from mutant mice (Fig. 1C). In addition, Western blot analysis with antibodies specific for PKBα and PKBβ, respectively, showed no compensatory upregulation of PKBα and/or PKBβ, respectively, in the brain of $Pkb\gamma^{-/-}$ mice (Fig. 1D).

Distribution of PKBγ in wild-type tissues

It has been reported that the PKBα and β isoform are widely expressed in all organs, but with some isoform-specific features (Altomare et al., 1998; Yang et al., 2003). Less is known about the tissue distribution of the PKBγ isoform. Previous reports suggest that PKBγ has a more restricted distribution with high levels in the adult brain and foetal heart and low levels in liver and skeletal muscle (Brodbeck et al., 1999; Masure et al., 1999; Yang et al., 2003). We assessed the distribution of PKBγ mRNA in 15 major tissues of adult mice by quantitative RT-PCR and normalised to the level of PKBγ in the brain (Fig. 2A). PKBγ mRNA was found at the highest level in brain and testis, and at lower levels in lung, mammary gland, fat and spleen.

To investigate whether PKBγ ablation leads to compensatory increase in PKBα and/or PKBβ, total RNA isolated from brain, testis, lung, mammary gland, fat and spleen of three *Pkbγ* wild-type and three mutant mice was subjected to quantitative RT-PCR. The levels of PKBα and β were normalised to the level of PKBα in wild-type brain and set as 100%. Overall, no marked upregulation of PKBα and/or PKBβ was observed, including the brain (Fig. 2B,C). These results are consistent with Western blot analysis of protein extracts of brains from *Pkbγ* wild-type and mutant mice (Fig. 1D). To investigate the distribution and levels of individual PKB isoforms within the brain, protein lysates were prepared from ten anatomically and functionally different regions. In general, all three isoforms were expressed in all examined regions but with certain isoform-specific features (Fig. 2D). PKBα is expressed in all regions at similar levels, whereas PKBβ is expressed at moderate levels in cortex, cerebellum, hippocampus and olfactory bulb, and at lower levels in the hypothalamus, midbrain, brain stem and spinal cord. PKBγ is expressed in all examined regions but at higher levels in the cortex and in the cerebellum.

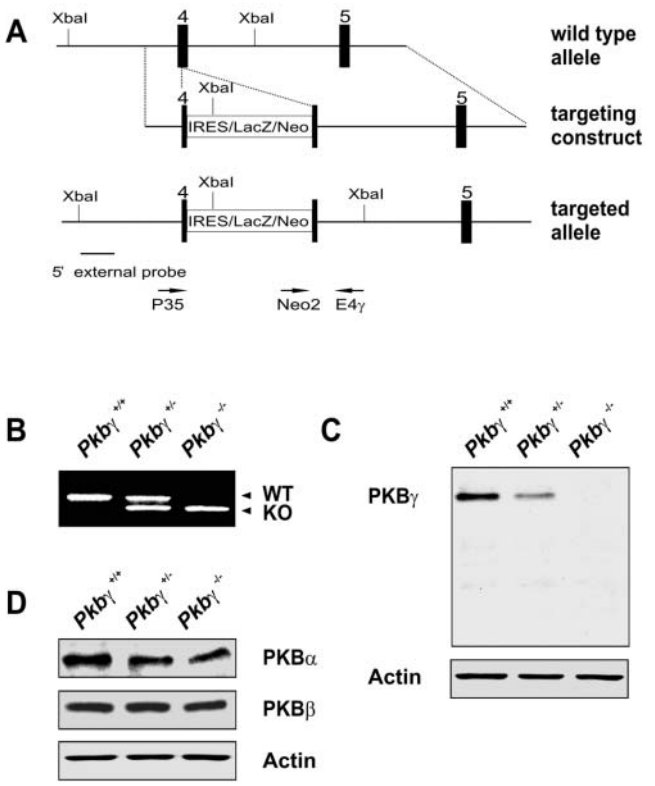

Fig. 1. Targeting strategy and confirmation of genotype. (A) The genomic organization of the *Pkbγ* wild-type allele (top) was disrupted using a targeting vector with an IRES-*lacZ*-Neo-cassette (middle). Targeting of the wild-type allele leads to disruption of exon 4 of the *Pkbγ* gene (bottom). Arrowheads indicate the localization of the primers for the PCR reaction. (B) The genotype of mice was determined by PCR. Representative results from $Pkb\gamma^{+/+}$, $Pkb\gamma^{+/-}$ and $Pkb\gamma^{-/-}$ mice are shown. (C) The levels of PKBγ in the brains of $Pkb\gamma^{+/+}$, $Pkb\gamma^{+/-}$ and $Pkb\gamma^{-/-}$ mice were determined by western blot analysis using a PKBγ-specific antibody. (D) The levels of PKBα and PKBβ, respectively, were determined in brain lysates from $Pkb\gamma^{+/+}$, $Pkb\gamma^{+/-}$ and $Pkb\gamma^{-/-}$ mice using PKBα- and PKBβ-specific antibodies.

Signalling in *Pkbγ* mutant mice

The phosphorylation/activation state of PKB in protein extracts from brains of 3-month-old $Pkb\gamma^{+/+}$ and $Pkb\gamma^{-/-}$ mice was analysed using an antibody specific for the phosphorylation site (anti-phospho-Ser-473) in the hydrophobic motif of the regulatory domain of all three isoforms (Fig. 3A). As expected, levels of activated PKB (quantification was done using actin as loading control) in $Pkb\gamma^{-/-}$ mice was significantly lower than in $Pkb\gamma^{+/+}$ littermate controls (100% versus 38%), but was not completely abolished (Fig. 3B). The phosphorylation levels of glycogen synthase kinase 3 (GSK3), tuberous sclerosis complex 2 (TSC2), p70S6K, ERK and p27 in $Pkb\gamma^{-/-}$ mice were not significantly changed when compared with wild-type littermate controls (levels of phosphorylated protein were normalised with the level of unphosphorylated protein). We repeated this experiment using brain samples of 14 days old mice and obtained comparable results with significantly reduced levels of total phosphorylated PKB and unchanged levels of phosphorylated substrates (data not shown).

Several recent studies emphasize the importance of insulin-like growth factor 1 (IGF1) signalling in the survival and proliferation of oligodendrocytes and myelination in the central nervous system (D'Ercole et al., 2002). Mice lacking IGF1 also have reduced brain weight and reduced size of the corpus callosum and anterior commissure (Ye et al., 2002). Therefore, we performed a western blot analysis with cell lineage-specific markers using antibodies against myelin basic protein (oligodendrocytes), glial fibrillary acidic protein

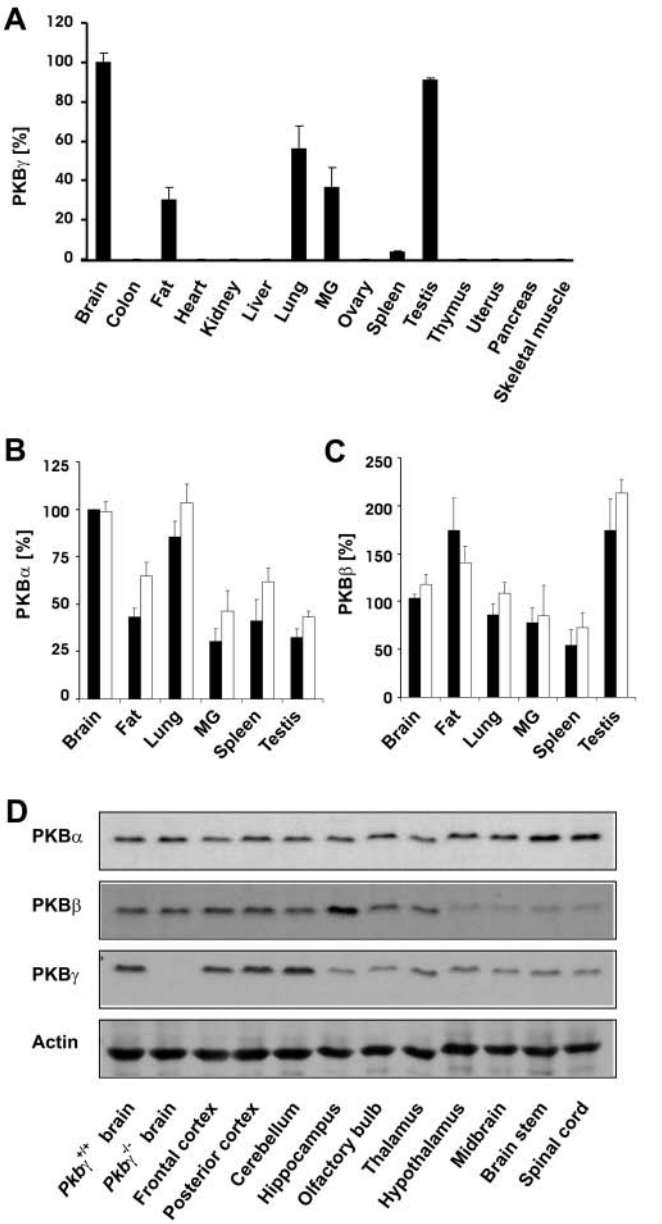

Fig. 2. Tissue distribution of PKBγ and levels of PKBα and PKBβ in *Pkbγ* mutant mice. (A) The mRNA level of PKBγ was determined in 15 different organs from adult $Pkb\gamma^{+/+}$ mice. Total RNA was isolated from three adult mice and the levels were normalized to the level of PKBγ in the brain (100%). MG, mammary gland. Error bars represent s.d. mRNA levels of (B) PKBα and (C) PKBβ were determined using total RNA from six different organs of adult *Pkbγ* wild-type (n=3; black bars) and mutant mice (n=3; white bars). mRNA levels of PKBα and PKBβ were normalized to the level of PKBα in wild-type brain (100%). Error bars represent s.d. (D) Western blot analysis of PKBα, β and γ within ten different brain regions using isoform specific antibodies.

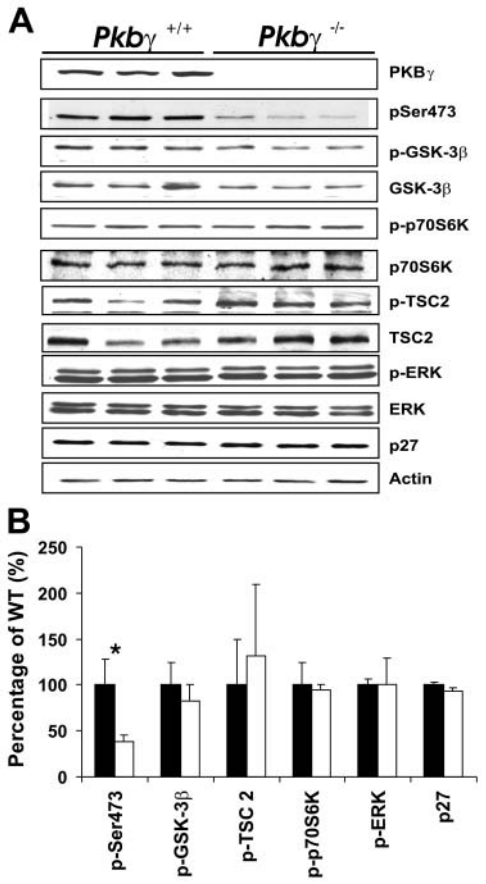

Fig. 3. Phospho-western blot analysis of brains from *Pkbγ* mutant mice. (A) Brains of three wild-type and three mutant mice were analysed for phosphorylation status of proteins involved in PKB signalling. p, indicates phosphorylated protein. (B) Western blot quantification. Levels of p-Ser473 and p27 were normalized to the level of actin, all phosphorylated proteins were normalized to the level of unphosphorylated protein. *P<0.05. Error bars represent s.d.

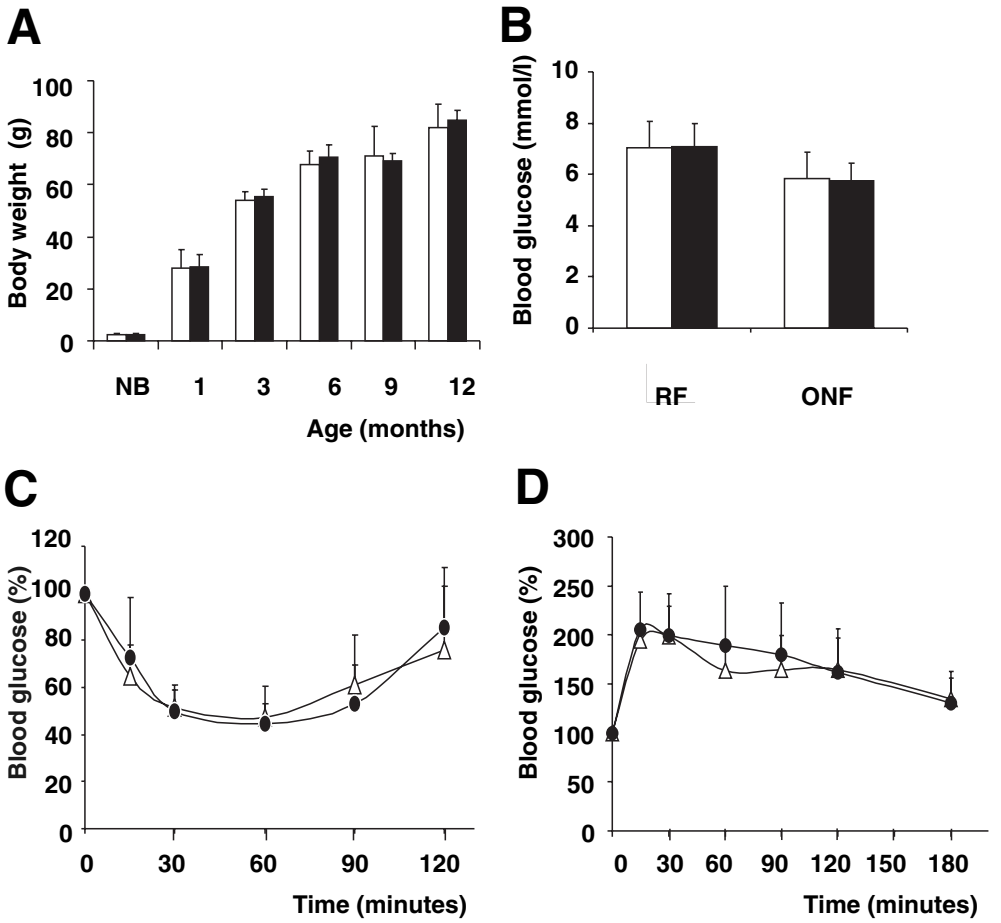

Fig. 4. Dispensable role of PKBγ for body weight and glucose metabolism. (A) Body weights of male $Pkb\gamma^{+/+}$ (white bars) and $Pkb\gamma^{-/-}$ (black bars) mice were measured at different points in time (n=5-8 animals per genotype). Error bars represent s.d. NB, newborn. (B) Blood glucose concentrations from random-fed (RF) and overnight fasted (ONF) mice (n=8; 6 months old; $Pkb\gamma^{+/+}$ white bars and $Pkb\gamma^{-/-}$ black bars). Error bars represent s.d. (C) Insulin tolerance test. Animals (n=6; 6 months old; $Pkb\gamma^{+/+}$ white triangles and $Pkb\gamma^{-/-}$ black circles) were fasted overnight and insulin (1 U/kg) was administered by intraperitoneal injection. (C) Glucose concentrations were determined at indicated time points from whole blood collected from tail veins. Values were normalized to the starting glucose concentration at the administration of insulin. Error bars represent s.d. (D) Glucose tolerance test. Animals (n=6; 5-6 months old; $Pkb\gamma^{+/+}$ white triangles and $Pkb\gamma^{-/-}$ black circles) were fasted overnight and glucose (2 g/kg) was orally administered. Blood glucose concentrations were sampled at the indicated times. Values were normalized to the starting glucose concentration at the administration of glucose. Error bars represent s.d.

(astrocytes) and M-neurofilaments (neurons). Significantly, no obvious differences in the expression levels of these marker proteins were observed when comparing samples of $Pkb\gamma^{+/+}$ and $Pkb\gamma^{-/-}$ mice (n=5 per genotype, data not shown).

PKBγ is not required for postnatal survival, fertility, body weight and glucose metabolism

There was no evidence for increased mortality of $Pkb\gamma^{-/-}$ mice after birth in an analysis of more than 400 pups (aged 3-4 weeks) [$Pkb\gamma^{+/+}$: $Pkb\gamma^{+/-}$: $Pkb\gamma^{-/-}$=104 (25.6%): 206 (50.7%): 96 (23.6%)]. As PKBγ is highly expressed in the testis, fertility of mutant mice was tested using male $Pkb\gamma^{-/-}$ × female $Pkb\gamma^{+/+}$ and female $Pkb\gamma^{-/-}$ × male $Pkb\gamma^{+/+}$ matings. Both male and female mutant mice matings gave normal pregnancies and births, indicating that fertility is not impaired in either male or female *Pkbγ* mutant mice (data not shown).

As PKB has been implicated in the regulation of cell and organ growth, body weight was measured in male *Pkbγ* mutant mice and wild-type littermate controls (n=5-8 per group) at different time points (Chen et al., 2001; Cho et al., 2001b; Peng et al., 2003; Yang et al., 2003). Body weight did not differ significantly between male *Pkbγ* mutant mice and wild-type controls at any time point (Fig. 4A). A similar result was obtained with female $Pkb\gamma^{-/-}$ mice and $Pkb\gamma^{+/+}$ controls (n=5-8 per group, data not shown), indicating that PKBγ does not play a significant role in the overall growth of mice.

To investigate a potential role of PKBγ in the regulation of glucose metabolism, blood glucose levels were measured in adult (5-6 months) *Pkbγ* mutant mice under random-fed and fasting condition, and compared with age- and gender-matched wild-type controls. Interestingly, both random-fed and fasting blood glucose levels, were not significantly different between wild-type and mutant mice (Fig. 4B). Additionally, blood insulin levels in random-fed condition did not differ significantly between $Pkb\gamma^{+/+}$ and $Pkb\gamma^{-/-}$ mice (1.32±0.08 μg/l versus 1.30±0.13 μg/l; n=6). To further investigate glucose metabolism, overnight fasted mice were challenged with insulin (insulin tolerance test) or glucose (glucose tolerance test). To test the insulin responsiveness, insulin (1 U/kg) was applied by intraperitoneal injection und blood glucose levels were measured at indicated time points using blood from tail veins. No obvious differences of blood glucose levels in the insulin tolerance test were found between the groups with mutant and control mice (Fig. 4C). Additionally, mice were challenged with orally applied glucose (2 g/kg) and blood glucose levels were measured at indicated time. Compared with wild-type mice, $Pkb\gamma^{-/-}$ mice displayed a very similar response to the glucose load (Fig. 4D). Taken together, these results suggest that PKBγ does not play a significant role in the maintenance of glucose homeostasis.

Essential role of PKBγ in postnatal brain development

Next, adult $Pkb\gamma^{+/+}$ and $Pkb\gamma^{-/-}$ mice were dissected and all major organs were investigated macroscopically. Compared with $Pkb\gamma^{+/+}$ littermate controls, the overall size of brains from

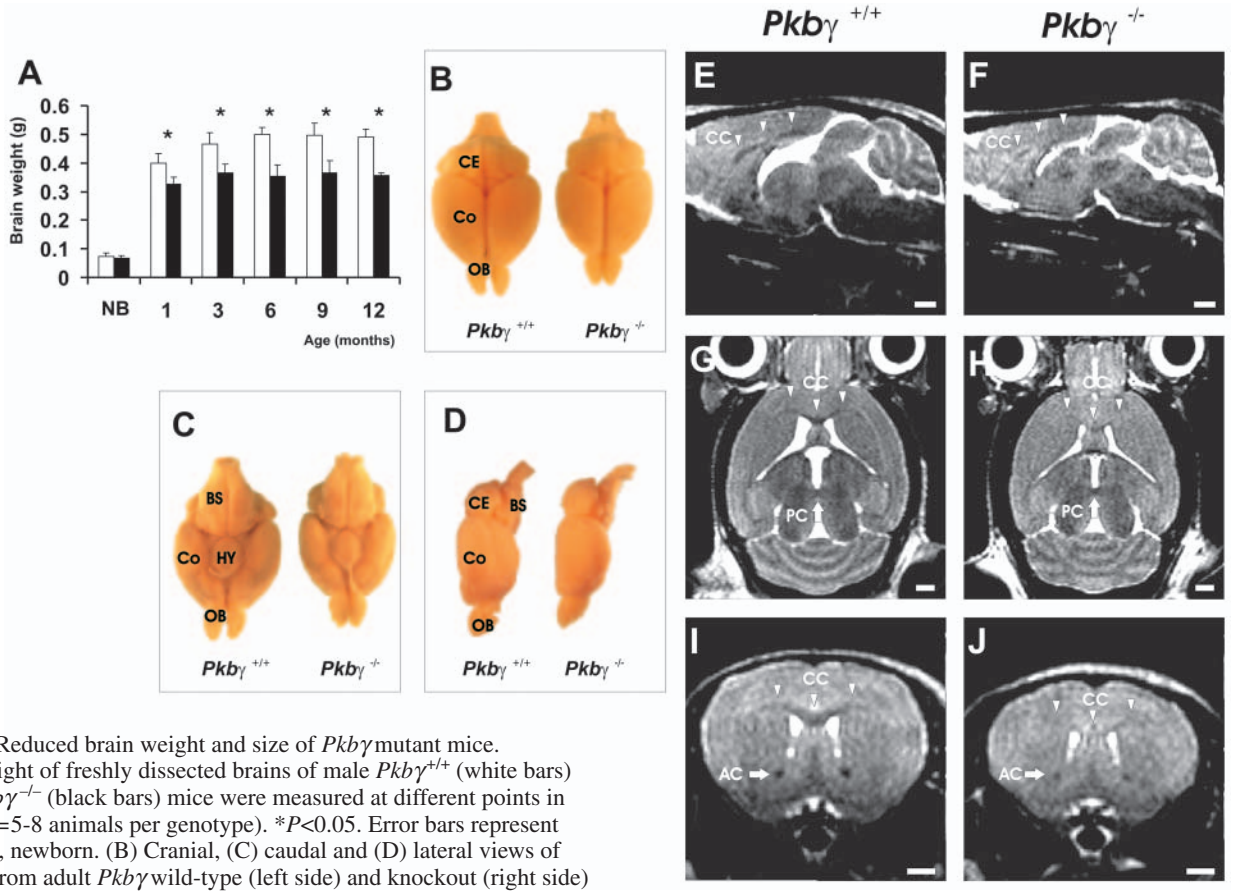

Fig. 5. Reduced brain weight and size of *Pkbγ* mutant mice. (A) Weight of freshly dissected brains of male *Pkbγ*$^{+/+}$ (white bars) and *Pkbγ*$^{-/-}$ (black bars) mice were measured at different points in time (n=5-8 animals per genotype). *P<0.05. Error bars represent s.d. NB, newborn. (B) Cranial, (C) caudal and (D) lateral views of brains from adult *Pkbγ* wild-type (left side) and knockout (right side) mice. Co, cortex; CE, cerebellum; OB, olfactory bulb; BS, brainstem; HY, hypothalamus. (E-J) Representative sections from T_2-weighted 3D MRI data sets acquired in vivo from the brains of *Pkbγ*$^{+/+}$ (E,G,I) and P*kbγ*$^{-/-}$ mice (F,H,J) from *Pkbγ*$^{+/-}$ matings in sagittal (E,F), horizontal (G,H) and coronal (I,J) orientation. CC, corpus callosum; AC, anterior commissure; PC, posterior commissure. Scale bar: 1 mm.

adult *Pkbγ*$^{-/-}$ mice was strikingly reduced. A representative example is shown in Fig. 5B-D. Furthermore, the weights of freshly dissected brains of *Pkbγ* wild-type and *Pkbγ* mutant mice were measured at different ages (Fig. 5A). Compared with age- and gender-matched wild-type littermate controls, brains from adult *Pkbγ*$^{-/-}$ mice (3-12 months old) exhibited a highly significant reduction in weight of about 25% (range 22%-29%), affecting both males and females (data for females not shown, n=5-8). Interestingly, at birth, brain weight did not differ significantly between *Pkbγ*$^{+/+}$ and *Pkbγ*$^{-/-}$ mice. The reduction in brain size and weight was first observed at the age of 1 month, but was less pronounced compared with adult mice (≈18%). In contrast to *Pkbα*, *Pkbβ* and *IgfI*-null mutant mice (Beck et al., 1995; Cheng et al., 1998; Garofalo et al., 2003; Powell-Braxton et al., 1993), the brain/body weight ratio of *Pkbγ* mutant mice was also significantly reduced to a similar extent.

In vivo magnetic resonance imaging (MRI) of *Pkbγ*$^{-/-}$ mice

MRI is an excellent non-invasive technique for studying brain anatomy in transgenic and mutant mice (Kooy et al., 2001; Natt et al., 2002). For further characterization of *Pkbγ* mutant brain anatomy, five adult female mutant and five age and gender matched wild-type littermate controls (with the same genetic background) from *Pkbγ*$^{+/-}$ matings were examined using high-resolution 3D MRI as previously described (Natt et al., 2002). Fig. 5E-J shows representative T_2-weighted images of *Pkbγ*$^{+/+}$ and *Pkbγ*$^{-/-}$ brains in a sagittal, horizontal, and coronal section orientation. Complementary in vivo volumetry based on T_1-weighted 3D MRI confirmed the much smaller brain size of all five *Pkbγ* mutant mice. Compared with wild-type littermates, whole brain volume in *Pkbγ*$^{-/-}$ mice was significantly reduced by about 24% (513±14 mm^3 versus 391±16 mm^3, P<0.01; n=5). Although several brain regions were affected, including olfactory bulb, cortex and hippocampal formation, no alteration in the structural organization of the brain was observed, confirming the macro-pathological findings. Moreover, because the volume of the ventricular spaces in *Pkbγ*$^{-/-}$ mice was reduced (7.85±2.2 mm^3 versus 5.55±2.8 mm^3) in proportion to that of the whole brain and MRI revealed no enlargement of the subarachnoid space, the occurrence of an internal or external hydrocephalus is excluded as a cause of reduced brain size. Interestingly, in contrast to any wild-type littermate controls, all five *Pkbγ*$^{-/-}$ mice presented with a marked thinning of the corpus callosum (downward arrowheads in Fig. 5E,F). White matter fibres connections are depicted as hypointense structures in T_2-weighted images. Although unequivocally identifiable in *Pkbγ*$^{+/+}$ mice (Fig. 5E,G,I), the corpus callosum is partly indistinguishable from surrounding grey matter in *Pkbγ*$^{-/-}$ mice (Fig. 5F,H,J). Anterior

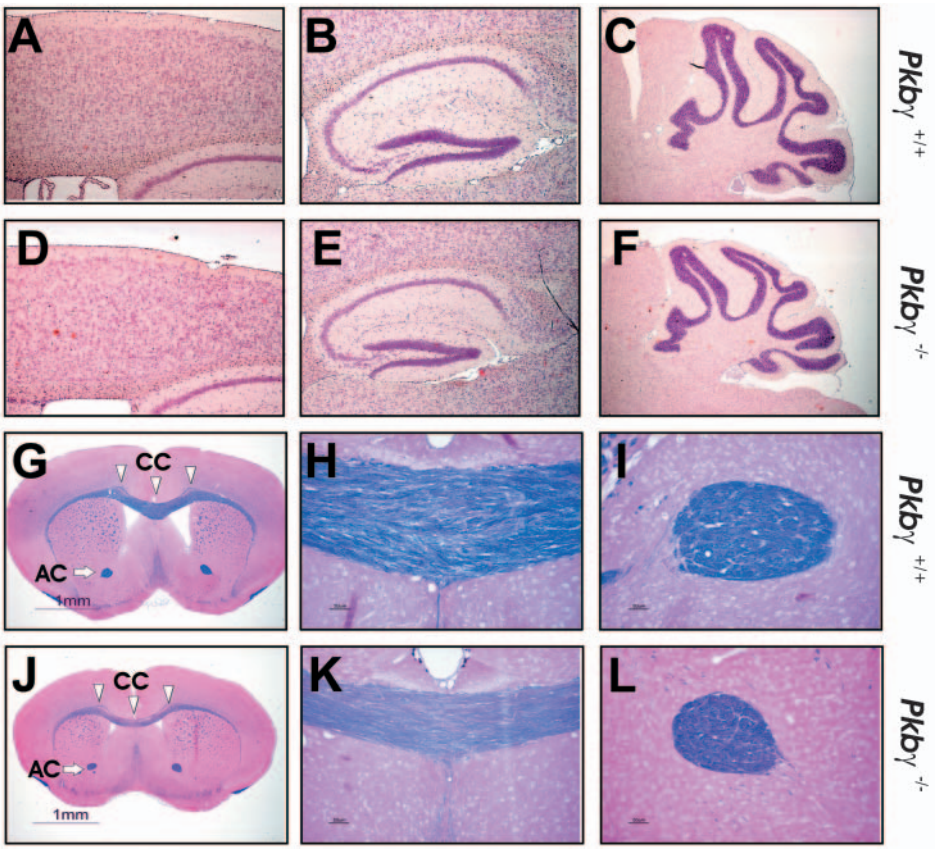

Fig. 6. Histology of brains from *Pkbγ* mutant mice. Representative sections (HE staining) of the cortex (A,D), hippocampus (B,E) and cerebellum (C,F) from adult $Pkb\gamma^{+/+}$ (A-C) and $Pkb\gamma^{-/-}$ (D-F) mice in parasagittal orientation. Representative sections stained for myelin (Luxol-Fast Blue/Eosin) of whole brain (G,J), corpus callosum (H,K) and anterior commissure (I,L) from $Pkb\gamma^{+/+}$ (G-I) and $Pkb\gamma^{-/-}$ mice (J-L) in coronal orientation. White matter structures are labelled as follows: CC, corpus callosum; AC, anterior commissure.

and posterior commissures as well as the hippocampal fimbria are less prominently affected.

Histology of $Pkb\gamma^{-/-}$ mouse brains

Histological examination of $Pkb\gamma^{-/-}$ brain was performed to investigate changes at the microscopic level. Various brain regions, including cerebellum, hippocampus and corpus callosum, were examined following Haematoxylin/Eosin staining (Fig. 6A-F). With the exception of the reduced size of all regions, no abnormalities in the overall structure of the different brain regions were observed. In line with the in vivo MRI findings, the thickness of the corpus callosum in *Pkbγ* mutant mice was markedly reduced (downward arrowheads in Fig. 6G,J). Additionally, myelin staining with luxol Fast Blue revealed not only a reduction in thickness of the corpus callosum but also less intense staining of the structure (Fig. 6H,K).

Cell number in the brains of $Pkb\gamma^{-/-}$ mice

Next, we indirectly assessed the cell number by measuring the amount of DNA in whole brains derived from $Pkb\gamma^{+/+}$ and $Pkb\gamma^{-/-}$ mice. The amount of DNA is considered as an indicator of cell number, whereas the amount of DNA per gram of tissue is an indicator of cell density which is reciprocal to cell volume (Zamenhof, 1976). The DNA contents of brains from newborns and 1-month-old mice were determined using the method described by Labarca and Paigen (Labarca and Paigen, 1980). Briefly, this method is based on the enhancement of fluorescence after binding of bisbenzimid to DNA. Compared with wild-type control samples, whole brain DNA content of $Pkb\gamma^{-/-}$ newborns did not differ significantly, indicating that cell number was not changed. Similarly, the DNA content per gram of brain tissue was comparable between *Pkbγ* wild-type and mutant mice, indicating a comparable cell size. In contrast to newborns, the DNA content in brains of 1-month-old *Pkbγ* mutant mice was slightly, but significantly, reduced compared with the $Pkb\gamma^{+/+}$ controls (Table 1). However, the DNA content per gram of tissue was, significantly increased in samples from $Pkb\gamma^{-/-}$ compared with wild-type littermate controls, indicative of increased cell density (and reduced cell size).

Additionally, the relative cell size in the posterior cortex of adult mice (3 months) was determined based on histological slides stained with DAPI. Cells were analysed using Image-Pro Plus in a defined field of view (≈1000 per field), and the area occupied by one cell was subsequently calculated. In line with the results of the DNA content experiment, the relative cell size was significantly and consistently reduced in *Pkbγ* mutant mice (100±10% versus 80±7%; n=5 per genotype; P<0.05). Taken together, the results show that both cell size and cell number contribute to the reduction in brain size observed in mutant mice, but the relative contribution of cell size reduction plays a more important part.

Susceptibility to glutamate and staurosporine induced cell death

It is established that the PI3K/PKB pathway plays a crucial role in cell survival in the central nervous system (Datta et al., 1999; Dudek et al., 1997; Kim et al., 2002). To investigate the potential role of PKBγ in apoptosis, primary cell cultures were established from $Pkb\gamma^{+/+}$ and $Pkb\gamma^{-/-}$ hippocampal neurons. Immunocytochemistry at day 28 using antibodies against tau (for axons) and Map2C (for dendrites) did not reveal any obvious defects in the differentiation of $Pkb\gamma^{-/-}$ hippocampal neurons (Fig. 7A-D). Consistent with the analysis of the expression pattern of PKB isoforms in various brain regions (Fig. 2D), we found that PKBα, PKBβ and PKBγ, respectively, were expressed in cultured wild-type primary hippocampal neurons. In accordance with the result of Fig. 1D, we did not

Table 1. Cell number in the brain of *Pkbγ* wild-type and mutant mice

	Age			
	Newborns		One month old	
	Pkbγ$^{+/+}$	Pkbγ$^{-/-}$	*Pkbγ*$^{+/+}$	*Pkbγ*$^{-/-}$
Body weight (g)	1.21±0.23	1.31±0.14 (107%)	14.1±2.5	13.0±2.3 (92%)
Brain weight (g)	0.071±0.001	0.069±0.006 (98%)	0.41±0.03	0.32±0.03 (78%)*
Brain/body weight ratio	0.059±0.011	0.054±0.008 (90%)	0.030±0.004	0.025±0.003 (85%)*
DNA/brain (mg)	0.59±0.04	0.56±0.12 (96%)	1.38±0.03	1.29±0.07 (93%)*
DNA/g of tissue (mg)	8.53±1.64	8.11±1.29 (95%)	3.38±0.20	4.04±0.47 (119%)*

The cell number in whole brains of *Pkbγ*$^{+/+}$ and *Pkbγ*$^{-/-}$ mice was determined in newborns and 1-month-old animals. Brain weight, brain/body weight and DNA content (parameter of cell number) per brain were significantly reduced in *Pkbγ*$^{-/-}$ mice at 1 month, but not in newborns. The DNA content per gram of tissue, a parameter of cell density, was significantly increased in *Pkbγ* mutant mice at 1 month, but not in newborns (*P<0.05).

find a compensatory upregulation of PKBα and PKBβ in *Pkbγ*-deficient cells (Fig. 7E). To test the potential role of PKBγ in the survival of hippocampal neurons, cell cultures were challenged with glutamate (15 mM/24 hours) or staurosporine (50 nM/12 hours) after 7 days in culture. Apoptotic cells were detected using the TUNEL assay. In untreated cells cultures, no significant difference in the percentage of apoptotic cells between *Pkbγ*$^{+/+}$ and *Pkbγ*$^{-/-}$ hippocampal neurons was observed (Fig. 7F). After treatment with glutamate or staurosporine, the percentage of apoptotic cells was significantly increased (51% and 24%, respectively, P<0.01) in cultures from *Pkbγ*$^{-/-}$ hippocampal neurons (Fig. 7F).

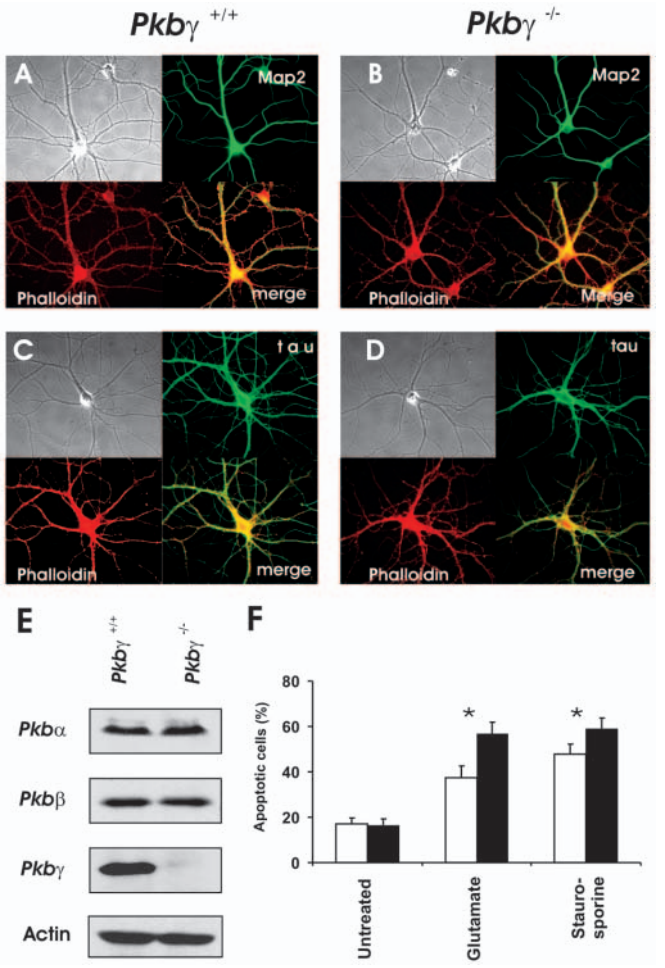

Additionally, we analysed the number of apoptotic cells from adult brains (n=5 per genotype) using TUNEL staining on parasagittal sections. Similar to the results of untreated cultures, we did not find any difference between *Pkbγ*$^{+/+}$ and *Pkbγ*$^{-/-}$ mice (data not shown).

Microarray analysis of *Pkbγ*$^{-/-}$ brains

In the CNS, a considerable amount of cellular and physiological events occur during postnatal development, such as neuronal outgrowth, differentiation, synaptogenesis and maturation. To investigate a potential role of PKBγ in these events, we analyzed gene expression patterns in brains of *Pkbγ*$^{+/+}$ and *Pkbγ*$^{-/-}$ mice at different time points during postnatal brain development, i.e. day 1, day 7 and day 30. RNA was extracted from whole mice brains and microarray analysis was performed on three individual brains per genotype and time point using murine Affymetrix GeneChips™. Changes below 1.5-fold increase were considered insignificant, and differentially regulated genes were subjected to a one-way ANOVA analysis (Table 2). As the brain consists of various heterogeneous cell populations, any change of expression occurring in a specific cell type will be quenched in the pool of whole brain RNA. It is therefore likely that the real expression changes in specific tissues are higher than apparent in this experiment. Among the 17,000 expressed genes, we found 37 genes to be differentially expressed in *Pkbγ*$^{-/-}$ brains versus *Pkbγ*$^{+/+}$ brains. Of these, 16 genes were upregulated and 21 genes downregulated. Among the genes with changed expression are several transcription factors and genes implicated in cell cycle and proliferation. Significantly, one of the most interesting findings is that at P30, several genes involved in synaptic transmission (pre- and postsynaptic), including ionotropic glutamate receptor (NMDAR1), potassium-chloride co-transporter 2 (KCC2), chapsyin 110 [channel-associated protein of synapses, 110 kDa (DLG2)] and

Fig. 7. Increased susceptibility to glutamate and staurosporine induced cell death. (A-D) Primary hippocampal neurons were established from E16.5 embryos and kept in culture for 28 days. Immunocytochemistry was performed using antibodies against dendritic (Map2C) or axonal (tau) proteins. (E) PKBα, PKBβ and PKBγ expression in *Pkbγ* wild-type and mutant hippocampal neurons. (F) Seven-day-old cultures were treated with glutamate (15 mM/24 hours) or with staurosporine (50 nM/12 hours) or were left untreated (*Pkbγ*$^{+/+}$ white bars and *Pkbγ*$^{-/-}$ black bars). Apoptotic cells were identified by TUNEL-assay and at least 200 cells per culture were counted (n=5 cultures per treatment and genotype). *P<0.05. Error bars represent s.d.

Table 2. Microarray analysis of Pkbγ mutant brain

Gene name	GenBank Accession Number	Fold change in expression: Day 1	Day 7	Day 30	Function
RIO kinase 3 (yeast)	AK004748	5.47*	0.59	1.52*	Chromatin condensation
Kinesin family member 5B	BF099632	2.24*	0.72	1.03	Microtubule based transport
Small EDRK-rich factor 1	AA709993	1.69*	1.14	1.06	
CD24a antigen	BB560574	1.57*	1.33	1.12	Cell proliferation
SRp20, splicing factor, arginine/serine-rich 3	AV135383	1.53*	1.32	0.91	mRNA splicing
WNK1 (protein kinase, lysine deficient 1)	BI692255	1.53*	1.00	0.93	Blood pressure
ATPase, Na^+/K^+ transporting, alpha 2 polypeptide	BQ175915	2.23*	2.93*	1.71*	Nt uptake, K^+ uptake
SRY-box containing gene 11	BG072739	0.96	1.82*	0.95	Transcription
Histone 1, H2af	W91024	1.04	1.60*	1.16	Nucleosome structure
Upstream transcription factor 1	AF479773	1.53*	1.55*	1.45	Transcription
Early B-cell factor 3	AK014058	1.13	1.54*	0.76	Transcription
RNA-binding region (RNP1, RRM) containing 2	BB436856	1.40	1.53*	1.46	Transcription
CDC28 protein kinase regulatory subunit 2	NM_025415	1.09	1.53*	1.20	Cell cycle
Procollagen, type III, alpha 1	BG968894	1.08	1.09	2.10*	Cell adhesion
Surfeit gene 4	AI788623	1.20	1.23	1.83*	Membrane protein
$GABA_A$ receptor, subunit alpha 6	NM_008068	1.06	0.57*	0.92	Synaptic transmission
ATPase, Na^+/K^+ transporting, alpha 2 polypeptide	AI845177	0.72	0.66*	0.56*	Nt uptake, K^+ uptake
Kinesin family member 5A	NM_008447	1.04	0.80	0.53*	Microtubule based transport
ADP-ribosylation factor 3	NM_007478	1.05	0.80	0.56*	Protein transport
Contactin associated protein 1	NM_016782	0.96	0.96	0.57*	Cell adhesion
Fibroblast growth factor 1	BM932451	0.86	0.95	0.59*	Angiogenesis, cell proliferation
Growth arrest specific 7	NM_008088	0.89	0.89	0.59*	Neurite outgrowth
Ca^{2+}/calmodulin-dependent protein kinase II alpha	X14836	1.04	0.69	0.59*	Cell cycle, synaptic plasticity
K^+/Cl^- co-transporter (KCC2/SLC12A5)	AF332064	1.13	0.90	0.62*	Synaptic transmission
Glutamate receptor, ionotropic, NMDA1 (ζ1)	NM_008169	0.96	0.80	0.63*	Synaptic transmission
Synaptotagmin 2	AF257304	1.02	1.00	0.64*	Synaptic transmission
Fascin homolog 1, actin bundling protein	BE952057	1.06	0.86	0.64*	Actin binding
Potassium voltage-gated channel, beta member 2	L48983	0.87	0.86	0.64*	Ion transport
Protein tyrosine phosphatase, receptor type, F	NM_011213	0.98	1.03	0.65*	Cell adhesion
Coronin, actin binding protein 1C	AW548837	0.97	0.94	0.65*	Actin assembly
Chapsyn-110 [discs, large homolog 2 (DLG2)]	BB622767	1.29	0.80	0.65*	Synaptic transmission

Genes with altered expression in male $Pkb\gamma^{-/-}$ mice (n=3) compared with $Pkb\gamma^{+/+}$ animals at different time points during postnatal brain development.
*Significant changes (1.5 fold).
Nt, neurotransmitter.

synaptotagmin 2 (SYT2), have significantly reduced expression levels in *Pkbγ* mutant brains. Additionally, Ca^{2+}/calmodulin-dependent protein kinase II α (CaMKII), an enzyme that is essential in synaptic plasticity and memory formation, was found at reduced expression levels (Ninan and Arancio, 2004).

Discussion

Here, we report the phenotypic consequences of the ablation of the *Pkbγ* gene. Mice with targeted disruption of all single PKB isoform were generated and all demonstrated a distinct phenotype. Mice deficient in *Pkbα* are smaller with a 30% reduction in body size and partial neonatal lethality, which might be caused by placental insufficiency (Chen et al., 2001; Cho et al., 2001b; Yang et al., 2003). By contrast, *Pkbβ* knockout mice exhibited a diabetes-like syndrome with hyperglycemia and impaired insulin action in fat, liver and skeletal muscle and, depending on the genetic background, mild growth retardation (Cho et al., 2001; Garofalo et al., 2003). Recently, Peng and colleagues reported the generation of *Pkbαβ* double mutant mice with severe intrauterine growth retardation that die shortly after birth with multiple defects in skin, bone and fat tissue (Peng et al., 2003). However, our results demonstrate that *Pkbγ*-deficient mice display a distinct phenotype without increased mortality, growth retardation and altered glucose homeostasis. Inactivation of the *Pkbγ* gene leads to a considerable reduction in total phosphorylated/activated PKB in the mutant brain without any compensatory increase of the α and β isoforms (assessed at the mRNA and protein levels), suggesting a failure to fully compensate for the loss of PKBγ. This result is consistent with findings in *Pkbα* and *Pkbβ* mutant mice, where no compensatory upregulation of 2 remaining isoforms was found (Cho et al., 2001b; Garofalo et al., 2003; Yang et al., 2003). It has been speculated that the distinct phenotypes of *Pkbα* and *Pkbβ* mutant mice are due to specific and distinct functions of the different PKB isoforms. By contrast, Peng and colleagues proposed that the individual phenotypes are due to loss of the dominant isoform in a specific tissue, which leads to significant reduction of total activated PKB below a crucial level (Peng et al., 2003). For example, the observed diabetes mellitus-like syndrome of $Pkb\beta^{-/-}$ mice could be due to ablation of the dominant isoform in the classical insulin-responsive tissues such as fat, liver and muscle. Moreover, the loss of a second isoform would have an additive effect in reducing the level of total PKB and, therefore, would intensify the phenotype. This possibility is supported by the observation of *Pkbαβ* double knockout mice (Peng et al., 2003) and our unpublished data on the *Pkbαγ* double mutant mice (Z.-Z.Y. and B.A.H., unpublished). Ablation of a single copy of *Pkbγ* in *Pkbα*-deficient mice ($Pkb\alpha^{-/-}$ $Pkb\gamma^{+/-}$) led to a higher perinatal mortality compared with *Pkbα* single mutant

mice and the ablation of both *Pkbγ* alleles in *Pkbα*$^{-/-}$ mice led to more pronounced dwarfism and intra-uterine death of all *Pkbα*$^{-/-}$*Pkbγ*$^{-/-}$ double mutant animals. However, it cannot be confirmed yet whether the observed phenotypes are due to a combination of reduced level of activated PKB and the loss of isoform-specific functions.

The IGF1/PI3K/PKB pathway plays a crucial role in mammalian brain development and function (D'Ercole et al., 2002; Rodgers and Theibert, 2002). Besides the severe growth retardation, adult mice with IGF1 deficiency exhibit a significant (38%) brain weight reduction (Beck et al., 1995). Similar to the *Pkbγ* mutant mice, all brain parts of the *Igf1*$^{-/-}$ mice were affected but the general anatomical organisation was normal. Furthermore, ablation of IGF1 resulted in a cell type-dependent loss of neurons, as well as a reduced total number of oligodendrocytes and hypomyelination (Beck et al., 1995; Ye et al., 2002). In addition, targeted deletion of IRS2 in mice also produced a pronounced brain growth deficiency, but in contrast to *Pkbγ* mutants, the reduction was already apparent during embryonic (E15.5) development (Schubert et al., 2003). By contrast, an increased brain mass was observed in mice overexpressing IGF1 (Mathews et al., 1988; Ye et al., 1995). Moreover, mice with brain-specific deletion of PTEN, a negative regulator of the PI3K/PKB pathway, exhibited an enlarged brain with seizures and ataxia resembling Lhermitte-Duclos disease (Backman et al., 2001; Kwon et al., 2001). Less is known about the consequences of *Pkbα* and *Pkbβ* inactivation for mouse brain development. Compared with *Pkbγ*$^{-/-}$ mice, adult *Pkbα* and *Pkbβ* mutant mice showed only a slight decrease in brain weight (Garofalo et al., 2003; Yang et al., 2004). In both *Pkbα* and *Pkbβ* mutant mice, no changes in the gross brain morphology were reported.

However, inactivation of the *Pkbγ* gene resulted in a significant reduction of brain weight and size. Interestingly, *Pkbγ* deficiency did not affect the general anatomical organization of the brain. In vivo 3D MRI and histological analysis excluded the absence of a specific brain region as the main cause of the weight reduction, consistent with the result of the broad expression profile among brain regions. More specifically, the proportionally reduced ventricular system rules out major disturbances in production, circulation and absorption of cerebrospinal fluid as a cause of reduced cell size/number in *Pkbγ*$^{-/-}$ mice. The biological relevance of the MRI signal alterations in white matter such as the corpus callosum requires further investigation. Nevertheless, it should be noted that the in vivo MRI results are consistent with a pronounced, but not complete, deficit in myelin deposition (Boretius, 2003), which is also strongly supported by the histological findings for myelin staining. In agreement with our results, mice deficient in IGF1, a potent activator of PKBγ, the myelin-rich white matter regions, including corpus callosum and anterior commissure, were overproportionally reduced by about 70% (Beck et al., 1995). By contrast, mice overexpressing IGF1 display an increased brain weight and the corpus callosum of the *Igf1* transgenic mice was increased in excess of proportionality (Carson et al., 1993).

The PI3-K/PKB signalling pathway plays a crucial role in the determination of cell size (Scanga et al., 2000; Shioi et al., 2002; Tuttle et al., 2001; Verdu et al., 1999). Results from transgenic mice overexpressing PKB show larger cardiac myocytes and thymocytes, or hypertrophy and hyperplasia in the pancreas (Kovacic et al., 2003; Mangi et al., 2003). An increase in neuronal soma size was observed in mice with brain-specific deletion of PTEN (Backman et al., 2001; Kwon et al., 2001). By contrast, the size of skeletal muscle cells in *Pkbαβ* double mutant mice was dramatically reduced (Peng et al., 2003). Our results show that both cell number and cell size are affected, but that reduced cell size contributes more than the reduced cell number. Additionally, it has been shown that the mTOR signalling pathway is also involved in the determination of cell size (Montagne et al., 1999; Oldham et al., 2000; Zhang et al., 2000). PKB modulates mTOR activity by phosphorylating TSC2, with a subsequent disruption of the TSC1-TSC2 interaction (Inoki et al., 2002; Potter et al., 2003).

Recent publications have linked PI3-K/PKB with synaptic plasticity and memory (Dash et al., 2004; Kelly and Lynch, 2000; Lin et al., 2001; Robles et al., 2003; Sanna et al., 2002). Wang and colleagues demonstrated that the A-type γ-aminobutyric acid receptors ($GABA_AR$), which mediate fast inhibitory synaptic transmission, is phosphorylated by PKB (Wang et al., 2003). Phosphorylation of $GABA_AR$ leads to an increased number of receptor on the cell membrane and an increased synaptic transmission. Additionally, Lin et al. established a role of the PI3-K/PKB pathway in fear conditioning in the amygdala (Lin et al., 2001). As we found several genes involved in neuronal circuit activity in our microarray experiment, future behavioural and electrophysiological studies of *Pkbγ* mutant brains will elucidate the specific role of PKBγ in synaptic transmission, learning and memory.

In summary, we have demonstrated that *Pkbγ*-deficient mice display a phenotype distinct from *Pkbα* and *Pkbβ* mutant mice. Our results provide novel insights into the physiological function of PKBγ and suggest a crucial role in postnatal brain development of mammals. Identification of PKBγ specific substrates involved in postnatal brain development is now of critical importance.

The authors thank Michael Leitges (Max-Planck-Institut für Experimentelle Endokrinologie, Hannover, Germany) for providing the IRES/*lacZ*/Neo targeting cassette. From the FMI we acknowledge J. F. Spetz and P. Kopp for ES cell culture and generation of chimera, D. Hynx for animal care, H. Brinkhaus for help with neuronal cell culture, E. Oakeley and H. Angliker for microarray analysis, M. Sticker for helpful advice in histology and R. Portmann for advice on Western blot quantification. O.T. is supported by the Novartis Stiftung für Medizinisch-Biologische Forschung, Z.Z.Y. is funded in part by a grant from Bundesamt für Bildung und Wissenschaft (BBW #98.0176) and B.D. by the Swiss Cancer League (KFS 1167-09-2001 and KFS 01002-02-2000). The Friedrich Miescher Institute for Biomedical Research is funded by the Novartis Research Foundation.

References

Alessi, D. R., Andjelkovic, M., Caudwell, B., Cron, P., Morrice, N., Cohen, P. and Hemmings, B. A. (1996). Mechanism of activation of protein kinase B by insulin and IGF-1. *EMBO J.* **15**, 6541-6551.

Alessi, D. R., Deak, M., Casamayor, A., Caudwell, F. B., Morrice, N., Norman, D. G., Gaffney, P., Reese, C. B., MacDougall, C. N., Harbison, D. et al. (1997). 3-Phosphoinositide-dependent protein kinase-1 (PDK1): structural and functional homology with the Drosophila DSTPK61 kinase. *Curr. Biol.* **7**, 776-789.

Altomare, D. A., Lyons, G. E., Mitsuuchi, Y., Cheng, J. Q. and Testa, J. R. (1998). Akt2 mRNA is highly expressed in embryonic brown fat and the AKT2 kinase is activated by insulin. *Oncogene* **16**, 2407-2411.

Backman, S. A., Stambolic, V., Suzuki, A., Haight, J., Elia, A., Pretorius, J., Tsao, M. S., Shannon, P., Bolon, B., Ivy, G. O. et al. (2001). Deletion of Pten in mouse brain causes seizures, ataxia and defects in soma size resembling Lhermitte-Duclos disease. *Nat. Genet.* **29**, 396-403.

Beck, K. D., Powell-Braxton, L., Widmer, H. R., Valverde, J. and Hefti, F. (1995). Igf1 gene disruption results in reduced brain size, CNS hypomyelination, and loss of hippocampal granule and striatal parvalbumin-containing neurons. *Neuron* **14**, 717-730.

Boretius, S., Merkler, D., Awn, N., Stadelmann, C., Natt, O., Watanabe, T., Michaelis, T., Frahms, J. and Brück, W. (2003). How do T1-, T2- and MT-weighted images reflect de- and remyelination? In vivo MRI of mice treated with the demyelinating neurotoxic agent cuprizone. *Proc. Intl. Soc. Magn. Reson. Med.* **12**, 280.

Brazil, D. P. and Hemmings, B. A. (2001). Ten years of protein kinase B signalling: a hard Akt to follow. *Trends Biochem. Sci.* **26**, 657-664.

Brodbeck, D., Cron, P. and Hemmings, B. A. (1999). A human protein kinase Bgamma with regulatory phosphorylation sites in the activation loop and in the C-terminal hydrophobic domain. *J. Biol. Chem.* **274**, 9133-9136.

Burgering, B. M. and Coffer, P. J. (1995). Protein kinase B (c-Akt) in phosphatidylinositol-3-OH kinase signal transduction. *Nature* **376**, 599-602.

Carson, M. J., Behringer, R. R., Brinster, R. L. and McMorris, F. A. (1993). Insulin-like growth factor I increases brain growth and central nervous system myelination in transgenic mice. *Neuron* **10**, 729-740.

Chan, T. O., Rittenhouse, S. E. and Tsichlis, P. N. (1999). AKT/PKB and other D3 phosphoinositide-regulated kinases: kinase activation by phosphoinositide-dependent phosphorylation. *Annu. Rev. Biochem.* **68**, 965-1014.

Chen, W. S., Xu, P. Z., Gottlob, K., Chen, M. L., Sokol, K., Shiyanova, T., Roninson, I., Weng, W., Suzuki, R., Tobe, K. et al. (2001). Growth retardation and increased apoptosis in mice with homozygous disruption of the Akt1 gene. *Genes Dev.* **15**, 2203-2208.

Cheng, C. M., Joncas, G., Reinhardt, R. R., Farrer, R., Quarles, R., Janssen, J., McDonald, M. P., Crawley, J. N., Powell-Braxton, L. and Bondy, C. A. (1998). Biochemical and morphometric analyses show that myelination in the insulin-like growth factor 1 null brain is proportionate to its neuronal composition. *J. Neurosci.* **18**, 5673-5681.

Cheng, J. Q., Godwin, A. K., Bellacosa, A., Taguchi, T., Franke, T. F., Hamilton, T. C., Tsichlis, P. N. and Testa, J. R. (1992). AKT2, a putative oncogene encoding a member of a subfamily of protein-serine/threonine kinases, is amplified in human ovarian carcinomas. *Proc. Natl. Acad. Sci. USA* **89**, 9267-9271.

Cho, H., Mu, J., Kim, J. K., Thorvaldsen, J. L., Chu, Q., Crenshaw, E. B., 3rd, Kaestner, K. H., Bartolomei, M. S., Shulman, G. I. and Birnbaum, M. J. (2001a). Insulin resistance and a diabetes mellitus-like syndrome in mice lacking the protein kinase Akt2 (PKB beta). *Science* **292**, 1728-1731.

Cho, H., Thorvaldsen, J. L., Chu, Q., Feng, F. and Birnbaum, M. J. (2001b). Akt1/PKBalpha is required for normal growth but dispensable for maintenance of glucose homeostasis in mice. *J. Biol. Chem.* **276**, 38349-38352.

Cross, D. A., Alessi, D. R., Cohen, P., Andjelkovich, M. and Hemmings, B. A. (1995). Inhibition of glycogen synthase kinase-3 by insulin mediated by protein kinase B. *Nature* **378**, 785-789.

Dash, P. K., Mach, S. A., Moody, M. R. and Moore, A. N. (2004). Performance in long-term memory tasks is augmented by a phosphorylated growth factor receptor fragment. *J. Neurosci. Res.* **77**, 205-216.

Datta, S. R., Brunet, A. and Greenberg, M. E. (1999). Cellular survival: a play in three Akts. *Genes Dev.* **13**, 2905-2927.

D'Ercole, A. J., Ye, P. and O'Kusky, J. R. (2002). Mutant mouse models of insulin-like growth factor actions in the central nervous system. *Neuropeptides* **36**, 209-220.

Dudek, H., Datta, S. R., Franke, T. F., Birnbaum, M. J., Yao, R., Cooper, G. M., Segal, R. A., Kaplan, D. R. and Greenberg, M. E. (1997). Regulation of neuronal survival by the serine-threonine protein kinase Akt. *Science* **275**, 661-665.

Franke, T. F., Yang, S. I., Chan, T. O., Datta, K., Kazlauskas, A., Morrison, D. K., Kaplan, D. R. and Tsichlis, P. N. (1995). The protein kinase encoded by the Akt proto-oncogene is a target of the PDGF-activated phosphatidylinositol 3-kinase. *Cell* **81**, 727-736.

Garofalo, R. S., Orena, S. J., Rafidi, K., Torchia, A. J., Stock, J. L., Hildebrandt, A. L., Coskran, T., Black, S. C., Brees, D. J., Wicks, J. R. et al. (2003). Severe diabetes, age-dependent loss of adipose tissue, and mild growth deficiency in mice lacking Akt2/PKB beta. *J. Clin. Invest.* **112**, 197-208.

Hanada, M., Feng, J. and Hemmings, B. A. (2004). Structure, regulation and function of PKB/AKT – a major therapeutic target. *Biochim. Biophys. Acta.* **1697**, 3-16.

Inoki, K., Li, Y., Zhu, T., Wu, J. and Guan, K. L. (2002). TSC2 is phosphorylated and inhibited by Akt and suppresses mTOR signalling. *Nat. Cell Biol.* **4**, 648-657.

Irizarry, R. A., Bolstad, B. M., Collin, F., Cope, L. M., Hobbs, B. and Speed, T. P. (2003). Summaries of Affymetrix GeneChip probe level data. *Nucleic Acids Res.* **31**, e15.

Jones, P. F., Jakubowicz, T. and Hemmings, B. A. (1991a). Molecular cloning of a second form of rac protein kinase. *Cell Regul.* **2**, 1001-1009.

Jones, P. F., Jakubowicz, T., Pitossi, F. J., Maurer, F. and Hemmings, B. A. (1991b). Molecular cloning and identification of a serine/threonine protein kinase of the second-messenger subfamily. *Proc. Natl. Acad. Sci. USA* **88**, 4171-4175.

Kandel, E. S. and Hay, N. (1999). The regulation and activities of the multifunctional serine/threonine kinase Akt/PKB. *Exp. Cell Res.* **253**, 210-229.

Kelly, A. and Lynch, M. A. (2000). Long-term potentiation in dentate gyrus of the rat is inhibited by the phosphoinositide 3-kinase inhibitor, wortmannin. *Neuropharmacology* **39**, 643-651.

Kim, A. H., Yano, H., Cho, H., Meyer, D., Monks, B., Margolis, B., Birnbaum, M. J. and Chao, M. V. (2002). Akt1 regulates a JNK scaffold during excitotoxic apoptosis. *Neuron* **35**, 697-709.

Kooy, R. F., Verhoye, M., Lemmon, V. and Van Der Linden, A. (2001). Brain studies of mouse models for neurogenetic disorders using in vivo magnetic resonance imaging (MRI). *Eur. J. Hum. Genet.* **9**, 153-159.

Kovacic, S., Soltys, C. L., Barr, A. J., Shiojima, I., Walsh, K. and Dyck, J. R. (2003). Akt activity negatively regulates phosphorylation of AMP-activated protein kinase in the heart. *J. Biol. Chem.* **278**, 39422-39427.

Kwon, C. H., Zhu, X., Zhang, J., Knoop, L. L., Tharp, R., Smeyne, R. J., Eberhart, C. G., Burger, P. C. and Baker, S. J. (2001). Pten regulates neuronal soma size: a mouse model of Lhermitte-Duclos disease. *Nat. Genet.* **29**, 404-411.

Labarca, C. and Paigen, K. (1980). A simple, rapid, and sensitive DNA assay procedure. *Anal. Biochem.* **102**, 344-352.

Lin, C. H., Yeh, S. H., Lu, K. T., Leu, T. H., Chang, W. C. and Gean, P. W. (2001). A role for the PI-3 kinase signaling pathway in fear conditioning and synaptic plasticity in the amygdala. *Neuron* **31**, 841-851.

Mangi, A. A., Noiseux, N., Kong, D., He, H., Rezvani, M., Ingwall, J. S. and Dzau, V. J. (2003). Mesenchymal stem cells modified with Akt prevent remodeling and restore performance of infarcted hearts. *Nat. Med.* **9**, 1195-1201.

Masure, S., Haefner, B., Wesselink, J. J., Hoefnagel, E., Mortier, E., Verhasselt, P., Tuytelaars, A., Gordon, R. and Richardson, A. (1999). Molecular cloning, expression and characterization of the human serine/threonine kinase Akt-3. *Eur. J. Biochem.* **265**, 353-360.

Mathews, L. S., Hammer, R. E., Behringer, R. R., D'Ercole, A. J., Bell, G. I., Brinster, R. L. and Palmiter, R. D. (1988). Growth enhancement of transgenic mice expressing human insulin-like growth factor I. *Endocrinology* **123**, 2827-2833.

Meier, R., Alessi, D. R., Cron, P., Andjelkovic, M. and Hemmings, B. A. (1997). Mitogenic activation, phosphorylation, and nuclear translocation of protein kinase Bbeta. *J. Biol. Chem.* **272**, 30491-30497.

Montagne, J., Stewart, M. J., Stocker, H., Hafen, E., Kozma, S. C. and Thomas, G. (1999). Drosophila S6 kinase: a regulator of cell size. *Science* **285**, 2126-2129.

Nakatani, K., Sakaue, H., Thompson, D. A., Weigel, R. J. and Roth, R. A. (1999). Identification of a human Akt3 (protein kinase B gamma) which contains the regulatory serine phosphorylation site. *Biochem. Biophys. Res. Commun.* **257**, 906-910.

Natt, O., Watanabe, T., Boretius, S., Radulovic, J., Frahm, J. and Michaelis, T. (2002). High-resolution 3D MRI of mouse brain reveals small cerebral structures in vivo. *J. Neurosci. Methods* **120**, 203-209.

Nicholson, K. M. and Anderson, N. G. (2002). The protein kinase B/Akt signalling pathway in human malignancy. *Cell Signal* **14**, 381-395.

Ninan, I. and Arancio, O. (2004). Presynaptic CaMKII is necessary for synaptic plasticity in cultured hippocampal neurons. *Neuron* **42**, 129-141.

Oldham, S., Montagne, J., Radimerski, T., Thomas, G. and Hafen, E. (2000). Genetic and biochemical characterization of dTOR, the Drosophila homolog of the target of rapamycin. *Genes Dev.* **14**, 2689-2694.

Peng, X. D., Xu, P. Z., Chen, M. L., Hahn-Windgassen, A., Skeen, J., Jacobs, J., Sundararajan, D., Chen, W. S., Crawford, S. E., Coleman, K. G. et al. (2003). Dwarfism, impaired skin development, skeletal muscle

atrophy, delayed bone development, and impeded adipogenesis in mice lacking Akt1 and Akt2. *Genes Dev.* **17**, 1352-1365.

Potter, C. J., Pedraza, L. G., Huang, H. and Xu, T. (2003). The tuberous sclerosis complex (TSC) pathway and mechanism of size control. *Biochem. Soc. Trans.* **31**, 584-586.

Powell-Braxton, L., Hollingshead, P., Warburton, C., Dowd, M., Pitts-Meek, S., Dalton, D., Gillett, N. and Stewart, T. A. (1993). IGF-I is required for normal embryonic growth in mice. *Genes Dev.* **7**, 2609-2617.

Robles, Y., Vivas-Mejia, P. E., Ortiz-Zuazaga, H. G., Felix, J., Ramos, X. and Pena de Ortiz, S. (2003). Hippocampal gene expression profiling in spatial discrimination learning. *Neurobiol. Learn Mem.* **80**, 80-95.

Rodgers, E. E. and Theibert, A. B. (2002). Functions of PI 3-kinase in development of the nervous system. *Int. J. Dev. Neurosci.* **20**, 187-197.

Sanna, P. P., Cammalleri, M., Berton, F., Simpson, C., Lutjens, R., Bloom, F. E. and Francesconi, W. (2002). Phosphatidylinositol 3-kinase is required for the expression but not for the induction or the maintenance of long-term potentiation in the hippocampal CA1 region. *J. Neurosci.* **22**, 3359-3365.

Scanga, S. E., Ruel, L., Binari, R. C., Snow, B., Stambolic, V., Bouchard, D., Peters, M., Calvieri, B., Mak, T. W., Woodgett, J. R. et al. (2000). The conserved PI3′K/PTEN/Akt signaling pathway regulates both cell size and survival in Drosophila. *Oncogene* **19**, 3971-3977.

Scheid, M. P. and Woodgett, J. R. (2001). PKB/AKT: functional insights from genetic models. *Nat. Rev. Mol. Cell Biol.* **2**, 760-768.

Schubert, M., Brazil, D. P., Burks, D. J., Kushner, J. A., Ye, J., Flint, C. L., Farhang-Fallah, J., Dikkes, P., Warot, X. M., Rio, C. et al. (2003). Insulin receptor substrate-2 deficiency impairs brain growth and promotes tau phosphorylation. *J. Neurosci.* **23**, 7084-7092.

Shioi, T., McMullen, J. R., Kang, P. M., Douglas, P. S., Obata, T., Franke, T. F., Cantley, L. C. and Izumo, S. (2002). Akt/protein kinase B promotes organ growth in transgenic mice. *Mol. Cell Biol.* **22**, 2799-2809.

Stokoe, D., Stephens, L. R., Copeland, T., Gaffney, P. R., Reese, C. B., Painter, G. F., Holmes, A. B., McCormick, F. and Hawkins, P. T. (1997). Dual role of phosphatidylinositol-3,4,5-trisphosphate in the activation of protein kinase B. *Science* **277**, 567-570.

Tuttle, R. L., Gill, N. S., Pugh, W., Lee, J. P., Koeberlein, B., Furth, E. E., Polonsky, K. S., Naji, A. and Birnbaum, M. J. (2001). Regulation of pancreatic beta-cell growth and survival by the serine/threonine protein kinase Akt1/PKBalpha. *Nat. Med.* **7**, 1133-1137.

Verdu, J., Buratovich, M. A., Wilder, E. L. and Birnbaum, M. J. (1999). Cell-autonomous regulation of cell and organ growth in Drosophila by Akt/PKB. *Nat. Cell Biol.* **1**, 500-506.

Wang, Q., Liu, L., Pei, L., Ju, W., Ahmadian, G., Lu, J., Wang, Y., Liu, F. and Wang, Y. T. (2003). Control of synaptic strength, a novel function of Akt. *Neuron* **38**, 915-928.

Yang, J., Cron, P., Good, V. M., Thompson, V., Hemmings, B. A. and Barford, D. (2002a). Crystal structure of an activated Akt/Protein Kinase B ternary complex with GSK3-peptide and AMP-PNP. *Nat. Struct. Biol.* **9**, 940-944.

Yang, J., Cron, P., Thompson, V., Good, V. M., Hess, D., Hemmings, B. A. and Barford, D. (2002b). Molecular mechanism for the regulation of protein kinase B/Akt by hydrophobic motif phosphorylation. *Mol. Cell* **9**, 1227-1240.

Yang, Z. Z., Tschopp, O., Hemmings-Mieszczak, M., Feng, J., Brodbeck, D., Perentes, E. and Hemmings, B. A. (2003). Protein kinase B alpha/Akt1 regulates placental development and fetal growth. *J. Biol. Chem.* **278**, 32124-32131.

Yang, Z. Z., Tschopp, O., Baudry, A., Dummler, B., Hynx, D. and Hemmings, B. A. (2004). Physiological functions of protein kinase B/Akt. *Biochem. Soc. Trans.* **32**, 350-354.

Ye, P., Carson, J. and D'Ercole, A. J. (1995). In vivo actions of insulin-like growth factor-I (IGF-I) on brain myelination: studies of IGF-I and IGF binding protein-1 (IGFBP-1) transgenic mice. *J. Neurosci.* **15**, 7344-7356.

Ye, P., Li, L., Richards, R. G., DiAugustine, R. P. and D'Ercole, A. J. (2002). Myelination is altered in insulin-like growth factor-I null mutant mice. *J. Neurosci.* **22**, 6041-6051.

Zamenhof, S. and van Marthens, E. (1976). Neonatal and adult brain parameters in mice selected for adult brain weight. *Dev. Psychobiol.* **9**, 587-593.

Zhang, H., Stallock, J. P., Ng, J. C., Reinhard, C. and Neufeld, T. P. (2000). Regulation of cellular growth by the Drosophila target of rapamycin dTOR. *Genes Dev.* **14**, 2712-2724.